Polyelectrolyte Monolayers at the Mica/Air Interface: Mechanically Induced Rearrangements and Monolayer Annealing

K. Lowack and C. A. Helm*

Institut für Physikalische Chemie, Johannes Gutenberg-Universität, Jakob-Welder Weg 11, D-55099 Mainz, Germany

Received July 12, 1994; Revised Manuscript Received January 3, 1995®

ABSTRACT: We have carried out a series of experiments on the mobility of a polyelectrolyte monolayer (thickness: 0.7 nm) in a nitrogen atmosphere with the surface force apparatus. If two polyelectrolyte monolayer covered surfaces come into contact, we observe a polyelectrolyte meniscus surrounding the contact area. After separation of the surfaces, a polyelectrolyte ring tracing the rim of the former contact area can be found. The monolayer anneals within minutes. (To observe the isolated monolayer, the optics of the surface forces apparatus had to be further developed.) From wetting and photobleaching experiments with fluorescent-labeled monolayers, we deduce that the annealing is a monolayer flux driven by the change in surface energy. We find that the relative humidity (rh) mainly influences the annealing time if rh ≤80%. However, at rh ≈ 100%, not a polyelectrolyte but a water meniscus is observed. Polyelectrolyte bilayers can be deformed plastically, yet they do not anneal.

Introduction

With the growing technical relevance of hydrophilic polymers together with the increasing trend toward miniaturization of all mechanical devices, one has to appreciate the difference between bulk and surface. Furthermore, it is important to realize that changes in the adjacent phase may affect the properties of surface polymers much stronger than they affect the bulk material.

It is far from obvious how the properties of a polymer change if a monolayer instead of the bulk phase is considered. The segment mobility may be very different. This is due to both to the change in topology and the change of the intermolecular forces. Some of the segment/segment interactions are replaced by the segment/substrate interactions.

Until now, the mobility of polymer monolayers was investigated mainly by observing the spreading behavior of a droplet of a viscous polymer, usually PDMS [poly(dimethylsiloxane)] on a surface.[1] A polymer monolayer surrounding the droplet was found whose density depended on the surface energy of the substrate and possibly on the viscosity of the polymer. A slip movement was suggested for the wetting behavior of polymer melts[2] and experimentally observed for a ≈100 nm thick polymer layer.[3] The physical argument is that it is less expensive to concentrate shear at the polymer/solid interface than to spread it over all the liquid. However, little work has been done on very thin polymer layers. The polymers are supposed to lay as coils at the interface.[4]

If the bulk material of a polymer is well below the glass point, rather sophisticated preparation techniques are necessary to prepare a monolayer of that polymer. Polyelectrolyte molecules dissolved in water adsorb to a surface, especially if the surface and the polyelectrolyte bear charges of opposite sign. If a suitable substrate is immersed into an aqueous polyelectrolyte solution of low ionic strength, then a 0.7–0.8 nm thick polyelectrolyte layer is adsorbed.[5] Therefore, one may hope to obtain an almost perfect monolayer by this technique.

We found in earlier work that the mobility of amphiphilic surfactants physisorbed to mica was greatly influenced by the relative humidity.[6] At high relative humidity, water was incorporated into the hydrophilic head groups; thus the binding to the mica was reduced and the surfactants were much more mobile. A similar effect is likely to occur with polyelectrolyte monolayers.

If one considers the stability of a monolayer on a substrate, it is convenient to discuss it in terms of surface energy. (Throughout the text, the following convention will be used: the *surface energy* per unit area of the solid/vapor interface is denoted by γ, which by definition is half the *adhesion energy*, this being the (positive) work done on separating two unit areas from contact in an inert atmosphere.[7]) If we follow the definition of de Gennes, the mica surface is a high-energy surface.[2] Such a surface has a pronounced tendency to adsorb some molecules in order to decrease the surface energy. Values like $\gamma_{SV} \approx 120-200$ mN/m (ref 8 and references therein) are reported for cleaving experiments of mica in room air. In experiments with the surface force apparatus (SFA), a surface energy of $\gamma_{SV} \approx 54-80$ mN/m[9] was observed; improved experimental procedures yield values of 130–170 mN/m,[8] comparable to the cleaving experiments.

In contrast, the surface energy of alkanes is rather low, since the intermolecular forces are the weak van der Waals forces. Between polar organic molecules, additional attractive hydrogen bond or dipole–dipole forces may act, yet those are rather weak, too.[7] Thus, considering the surface energy, it is favorable if an organic monolayer covers a mica surface.

However, the situation is very different if two monolayer-covered surfaces come into contact. As before, the system tries to minimize its free energy. Thermodynamically, this is achieved by increasing the work of adhesion. Obviously, this can be achieved by removing the monolayers partly or completely out of the contact area and allowing the original high-energy surfaces to contact.

Yet, in any real experiment, one has to consider the less fundamental, but practically important, stress distribution within the contact area. The JKR theory[10] has successfully described the deformation of two ad-

* To whom correspondence should be addressed.
® Abstract published in *Advance ACS Abstracts,* March 1, 1995.

0024-9297/95/2228-2912$09.00/0

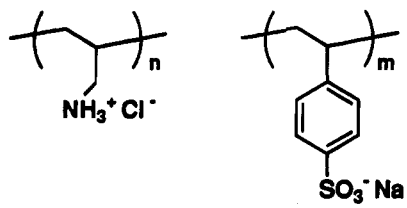

Figure 1. Chemical structures of the monomer units of the two polyelectrolytes used: positively charged PAH and negatively charged PSS.

hesive surfaces in a sphere-on-a-flat geometry, equivalent to the crossed cylinder configuration used in the SFA.[11] According to this theory, the largest compressive stresses are found in the center of the contact area, while the edges are subject to the largest tensile stresses. If we change the vapor content of the air (increase the relative humidity), the adhesion as well as the stress distribution between the surfaces may be substantially affected by capillary condensation.[7]

To shed some light on the situation, we have carried out a series of experiments to characterize the dynamic behavior of a polyelectrolyte monolayer on mica. We investigated the polyelectrolyte rearrangement occurring if two surfaces covered with such monolayers come into contact. After separation, we observed the annealing of an isolated monolayer. Finally, to verify our assumptions about monolayer mobility and the crucial role of the surface energy, we investigated a polyelectrolyte bilayer consisting of consecutively adsorbed polycations and polyanions. Our interpreation of the monolayer movement is further supported by photobleaching and wetting experiments.

Materials and Methods

The positively charged poly(allylamine) hydrochloride (PAH, M_w = 50 000–60 000) and the negatively charged poly(styrenesulfonate) sodium salt (PSS, $M_w \approx$ 70 000) were obtained from Aldrich (Sternheim, Germany). The chemical structures of the monomer units are shown in Figure 1. PAH was used without further purification. To remove PSS molecules of a low degree of polymerization, the material was dialyzed against water: An aqueous PSS solution was dialyzed for 2 days in a dialysis tube (VISKING 27132, Roth, Germany) and subsequently freeze-dried. Water was filtered in a Milli-Q unit and then distilled from $KMnO_4$ solution.

PAH was labeled with FITC (fluorescein isothiocyanate) (Sigma, München, Germany) according to a standard protein label process:[12] 20 mg of PAH and 0.2 mg of FITC were stirred in the dark for 2 h in 2.5 mL of a carbonate buffer solution of pH 9.5. Then the polymer was purified by gel filtration over a PD-10 column and subsequently freeze-dried. By considering the absorption of the solution, one finds that 1 in 400 monomer units is labeled; this corresponds to one labeled monomer unit per chain.

A PAH monolayer on mica was prepared by immersing a mica sheet in a 0.01 mol/L PAH aqueous solution. After 0.5 h the mica was retracted, thoroughly rinsed, and dried by a gentle stream of nitrogen. However, when Aldrich synthesized a new batch of PAH it was necessary to decrease the pH of the polyelectrolyte solution to 2.5–3 with HCl. Then it was possible to observe the monolayer movement described below. To prepare a polymer bilayer, the PAH-covered mica sheet was immersed for another 30 min in a 0.01 mol/L PSS aqueous solution; then the rinsing and drying was repeated.

The surface force apparatus (SFA) (Mark 4, ANUTECH, Australia) is a well-established tool for investigating the interaction of surfaces.[7,13] We chose a spring constant of K = 7 × 10^6 mN/m. To establish a low water content in the polymer layer, a small Petri dish with P_2O_5 was inserted at the bottom of the SFA. Prior to the experiments, the SFA was flushed for 1 h with dry nitrogen. Then the surfaces were allowed to equilibrate for 12–16 h. The relative humidity was changed by replacing the P_2O_5 with other salts (NaCl: rh = 30%; $(NH_4)_2SO_4$: rh = 80%; water: 100%). After the relative humidity was changed, the surfaces were allowed to equilibrate for another 12 h.

The silvered mica sheets form an optical cavity; only those wavelengths which interfere constructively are transmitted. Behind the interferometer a microscope objective (magnification 5) focuses the transmitted light on the entrance slit of a spectrograph (HR 320S *f*/4.2, Instruments S.A., Riber-Jobin-Yvon, Grasbrunn, Germany; grating 1200 grooves/mm), which is ≈500 mm away from the interferometer, thus leading to a magnification factor of ≈25. Behind the spectrograph a light-sensitive camera (Proxitronic, HL 5, Bensheim, Germany) with an image intensifier (Argus 10, Hamamatsu, Germering, Germany) with an image intensifier (Argus 10, Hamamatsu, Germering, Germany) and a video system allow the observation and recording of the fringe pattern, which gives basically a cross-cut of the interacting surfaces. For calibration purposes, a mercury pen-ray lamp is used.

In order to measure the thickness of the thin layer trapped between the surfaces, at the end of some experiments the organic layer was removed from the surfaces by UV degradation and desorption, following the procedure described before.[14] The UV pen lamp with wavelength 254 nm was bought from Oriel (Stratford, CT).

Contact-angle measurements were performed using the sessile drop technique (Kontaktwinkelmessgerät G1, Krüss, Hamburg, Germany). Both the advancing and the receding contact angles were measured. The surface tension of the aqueous solutions was determined by the Wilhelmy technique (WS1, Riegler & Kirstein, Wiesbaden, Germany).

The photobleaching experiments were carried out with a microscope (Axiotron, Zeiss, Göttingen, Germany) in the fluorescence configuration. The light source is a high-pressure mercury vapor lamp (50 W); the sample is illuminated with blue light ($\lambda \leq$ 490 nm). The filter system between the sample and the ocular ensures that only the emitted light with wavelengths above 500 nm serves to characterize the sample. The same camera, intensifier, and video system as for the SFA are employed to record the microscope pictures.

Optical Theory

We detect the remnants of a polyelectrolyte meniscus sitting on the polyelectrolyte monolayer, since the polyelectrolyte and the air have different refractive indices. While it is well known how to describe local changes in the refractive index when capillary condensation or cavities occur,[15] it was not necessary before to describe such changes when the surfaces were separated. Therefore, we shall give here the qualitative argument; a quantitative derivation may be found in the Appendix.

Within the cavity, the resonance wavelengths form standing waves, which are called fringes of equal chromatic order (FECO). If one considers a fringe of a given order, its wavelength is shortest when the mica sheets are in contact:[13,16]

$$m\lambda^0{}_m = 4n_{GI}D_{GI} \qquad (1)$$

m is the order of the resonance wavelength λ_m, which we call $\lambda^0{}_m$, if the surfaces contact, n_{G1} is the index of refraction of the mica, and D_{G1} is the thickness of one mica sheet. If the distance D between the surfaces is increased, the wavelength of the fringe is shifted toward the red; i.e., $\lambda_m = \lambda^0{}_m + \Delta\lambda_m$. For very small distances between the surfaces, the shift of the resonance wavelength $\Delta\lambda_m$ depends very strongly on the electrical field of the standing wave in the gap between the mica sheets. Due to the equal thickness of the mica sheets, this gap and the adjacent mica/air interfaces are just

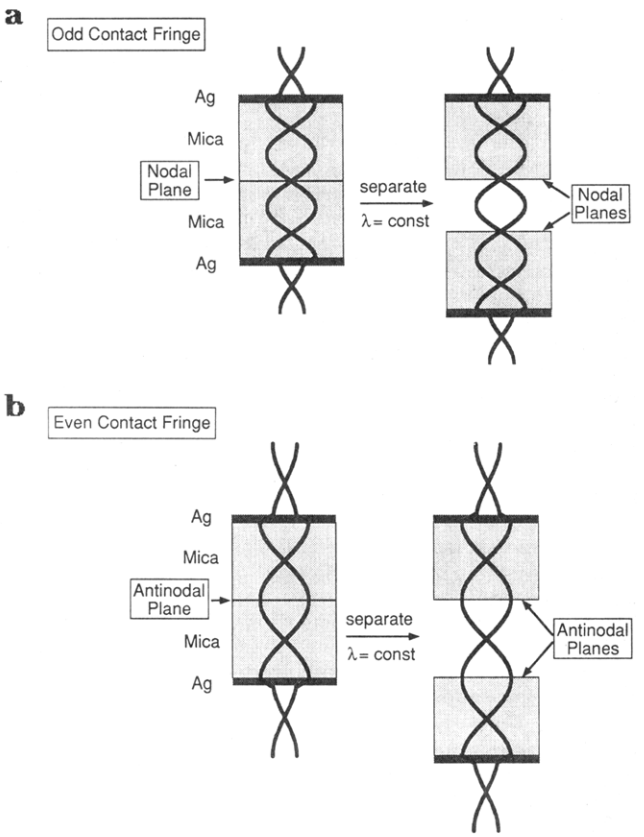

Figure 2. Electric field of standing waves within a cavity, as used in the SFA. (a) An odd ((b) an even) contact fringe with $m = 3$ ($m = 2$) is shown; due to the equal thickness of the mica sheets there is a nodal (antinodal) plane at the mica/mica interface. Also sketched are separated surfaces, where the wavelength of the higher order fringe $M = 4$ ($M = 3$) coincides with the contact wavelength. If the wavelength is the one of an odd (even) contact fringe, the electrical field at the medium/mica interface will have a node (an antinode), independent of the order of the fringe.

at the center of the cavity. There, the electrical field is naught (odd-order fringes) or its absolute value is at a maximum (even-order fringes). We find for a thin layer that the refractive index n of the medium between the mica sheets influences the resonance wavelength only if there is a light field at the position of the medium

$$D = \frac{m\Delta\lambda_m}{2n_{Gl}}, \qquad m \text{ odd} \tag{2}$$

and

$$D = \frac{m\Delta\lambda_m n_{Gl}}{2n^2}, \qquad m \text{ even} \tag{3}$$

If a water meniscus surrounds the contacting surfaces, it can be detected as a break in the even fringe, since air and water have different refractive indices. However, the odd contact fringes appear to be homogeneous, since the shift of the odd fringes is independent of the refractive index of the medium.

Equations 2 and 3 were derived for a symmetrical three-layer interferometer. However, if the monolayer-covered surfaces are separated, they constitute a symmetric five-layer interferometer (mica/monolayer/air/monolayer/mica). Still, most important for the shift of the fringes is the distribution of the electrical field,[16] which is shown schematically in Figure 2. Let us consider the contact wavelength λ^0_m. If the m fringe is an even fringe, the light field will have a maximum at the mica/mica interface if the surfaces contact. If the surfaces are separated so far that some higher order fringe coincides with λ^0_m, the light field will still have a maximum at the mica surfaces, since the optical path in the mica will be unchanged. Similarly, if λ^0_m is the contact wavelength of an odd fringe, a standing wave with wavelength λ^0_m and order M will have zero intensity at the mica surfaces.

If such a fringe of order M does not coincide perfectly with λ^0_m, i.e., $\lambda_M = \lambda^0_m + \partial\lambda$ (with $M > m$ and $\partial\lambda \ll \lambda^0_m$), then the distance D between the surfaces is given by

$$D \approx \frac{\lambda^0_m}{2n}(M - m) \tag{4}$$

(In laboratory lingo: "The surfaces are separated by ($M - m$) fringes.") Let us consider our experimental conditions: We define D_0 as a small correction to the air gap D as defined in eq 4, and D_F is the thickness of a thin polyelectrolyte film ($D_F \ll \lambda^0_m$) with refractive index n_F adsorbed onto the mica surfaces. Then we can derive the following relationships (for details, see the Appendix):

$$m\frac{\partial\lambda}{2n_{Gl}} = D_0 + 2D_F, \qquad m \text{ odd} \tag{5}$$

and

$$m\frac{\partial\lambda}{2}n_{Gl} = D_0 n^2 + 2D_F n_F^2, \qquad m \text{ even} \tag{6}$$

This approximation works best for low m and $M - m = 1$. Note that the refractive index of the thin film does not influence the wavelength shift for wavelengths which almost coincide with odd contact fringes, since the light field is zero at the position of the thin film. Now, let us consider the case when the film thickness D_F is increased by a certain (small) amount to $D_F + \Delta$. Since the distance between the mica surfaces remains constant, the air gap will be decreased to $D - 2\Delta$. As demonstrated by eq 5, the shift $\partial\lambda$ for those wavelengths which coincide with odd contact fringes depends on $2(D_F + \Delta) + (D_0 - 2\Delta) = 2D_F + D_0$. Thus, the change in composition at a position where the light field is zero does not affect the resonance wavelength.

In contrast, when the light field undergoes enhancement at the position of the thin film, a change of the film thickness to $D_F + \Delta$ will change $\partial\lambda$ to $\partial\lambda'$

$$m\frac{n_{Gl}}{2}\partial\lambda' = (D_0 - 2\Delta)n^2 + 2(D_F + \Delta)n_F^2$$
$$= m\frac{n_{Gl}}{2}\partial\lambda + 2\Delta(n_F^2 - n^2), \qquad m \text{ even} \tag{7}$$

Thus, lateral distributions of the film height (both the film height and its variations are supposed to be small) will be detected when the light field is enhanced at the position of the thin film. This is the case for all those fringes whose wavelength almost coincides with even contact fringes.

Results and Discussion

To characterize the interaction of the polyelectrolytes with water, the surface tension of PAH solutions and the contact angle with polyelectrolyte-covered mica were measured. With polymers adsorbed onto mica, we first

demonstrate that we actually deal with a monolayer. This was done by measuring the thickness of the adsorbed layer. Second, we shall describe how we observe the movement of a polyelectrolyte monolayer in the SFA, both rearrangements of contacting monolayers and annealing of an isolated monolayer. Then we discuss the pronounced influence of humidity on the monolayer mobility. To gain insight into the nature of the monolayer movement, wetting experiments with mica sheets half immersed into polyelectrolyte solutions as well as photobleaching experiments on fluorescence-labeled polyelectrolyte layers are performed. Finally, we describe the movements of a polyelectrolyte bilayer consisting of PAH and PSS on top.

Contact Angle and Surface Tension. Comparing the surface tension of pure water with the one of a 0.01 mol/L polyelectrolyte solutions, we found no effect. Therefore we conclude that almost no polyelectrolyte molecules adsorb at the air/water interface.

The contact angle between water and a PAH monolayer on mica was measured. On advancing, we found $\theta_a = 17.5 \pm 2.5°$ (stick-slip movement), on receding, $\theta_r = 0°$; i.e., the polyelectrolyte monolayer is quite hydrophilic, and also it appears to be rough on a molecular level. As soon as the polyelectrolyte monolayer is exposed to water, it will behave like the adsorbed polymer layer it originally was, with chains protruding into the water, etc. Such molecular rearrangements lead to a pronounced contact angle hysteresis.

Thickness of the Polyelectrolyte Monolayer. To estimate the thickness of the adsorbed polymer film, a droplet of 0.01 mol/L PAH aqueous solution was placed between the mica surfaces in in the SFA. After 0.5 h of equilibration time, the surfaces were pressed together until a flattening of the fringes similar as in air was obtained. These high compressive pressures overcome the repulsive hydration force;[7] the thickness of the layer trapped between the mica surfaces was estimated to be 1.4−1.6 nm. This corresponds to one adsorbed monolayer (0.7−0.8 nm) on each mica surface. This thickness agrees well with X-ray experiments on the buildup of polyelectrolyte multilayers.[5]

Mobility of the Polyelectrolyte Monolayer in Air. A typical measurement sequence is shown in Figure 3. At the top, spectrograms of the FECO fringe pattern are shown when the surfaces are brought into contact and no load is applied. The even fringe (the one on the right) appears to be broken slightly above and below the straight line. Scanning the surfaces, one finds this break of the even fringe surrounds the contact area.

Such a break of the even fringe is observed when the index of refraction changes discontinuously. First it was observed at high relative humidities when a water meniscus surrounds the contact area due to capillary condensation.[15] However, the experiments shown in the left column of Figure 3 were performed at rh $\approx$ 0%. Thus, we may assume that the rim surrounding the contact area consists mainly of polyelectrolyte.

In the second row in Figure 3, the contact area is decreased by a tensile load. The break of the even fringes stays at the edge of the contact area, independent of the velocity decreasing (or increasing) the applied load. According to the JKR theory,[10] the surfaces will spontaneously jump apart if the radius of the contact area is reduced to $0.63a_0$ (a_0 is the radius of the contact area when no load is applied). As is obvious from the left and center columns of Figure 3, the contact radius can be reduced to about $0.44a_0$, indicating that the adhesion of the surfaces is determined by more effects than simple JKR theory considers. The movement of the surfaces is rather sluggish; if one applies a tensile load sufficient to separate the surfaces, one has to wait about a second while the contact area decreases until the surfaces eventually jump apart.

After separating the surfaces, the distance between the surfaces was adjusted, so that they were separated by exactly "one or two fringes". The fringe pattern thus obtained is shown in the center row of Figure 3. Looking at the fringe on the right, whose wavelength is close to the one of the even contact fringe, we find little black holes, whereas the other fringe appears to be homogeneous. The holes are positioned exactly where the polymer meniscus was when the surfaces jumped apart. This can be verified especially well if one compares the photos in the second and the center rows. The (fuzzy, i.e., not time averaged) photos in the second row are taken just before the surfaces jumped. The diameter of the contact area at pull-off is identical to the distance between the black holes in the photographs in the center row. Scanning over the fringe, one finds that the boundary of the former contact area is now marked by a black rim.

Measuring the height of the polymer annulus when the surfaces contact as well as the width of the black holes, we may deduce that the polymer annulus is $\approx$5 $\pm$ 2 nm high and 6 $\pm$ 1 μm wide at 0% rh. If the surfaces are separated, this polyelectrolyte meniscus is ruptured. The chain molecules will protrude arbitrarily from the polyelectrolyte ring sitting on the surfaces. The roughness of the top of the ring reduces the reflected intensity of the standing waves whose light field is at a maximum, and the reflection from the top of the rim cannot be detected.

We can obtain an upper limit for the height of the ring, since the fringes which have almost the same wavelengths as the odd contact fringes appear homogeneous. The experimental data are $\lambda^0_m \approx 564.3$ nm, $m = 37$, and $n_F \approx 1.6$.[17] Comparing eq 5 with the exact solution, eq A1, we find that the approximation is very good for film thicknesses below 20 nm. Above that value, the index of refraction of the medium starts to influence the wavelength of the fringe by more than 0.1 nm; such a shift in the fringe can be easily resolved with the video system. For optical reasons, we can conclude that the thickness of the polymer ring sitting on the polyelectrolyte surface is below 10 nm.

After several minutes, the holes appear to be less black, yet sustain their shape. The exact annealing time depends on the humidity (to be discussed later) and the fringes appear to be continuous again; i.e., the polyelectrolyte ring protruding from the surfaces has disappeared. We have to conclude that all the chain molecules have burrowed back into the monolayer.

The bottom photos show the surfaces back in contact; again the polyelectrolyte meniscus forms. On separation we find again the black holes in the fringes which undergo field enhancement at the mica surface. The black holes disappear with time as described above. This can be repeated several times. The surfaces were left in contact for about 2 h; this, too, had no effect.

Figure 4 shows the fringe patterns which occur if the surfaces are brought into contact before the polyelectrolyte rings are allowed to anneal. For at most 40 ms, the fringes do not appear to be straight. Both the even and the odd fringes bulge back for a few fractions of a second and wiggle a bit; then the polyelectrolyte me-

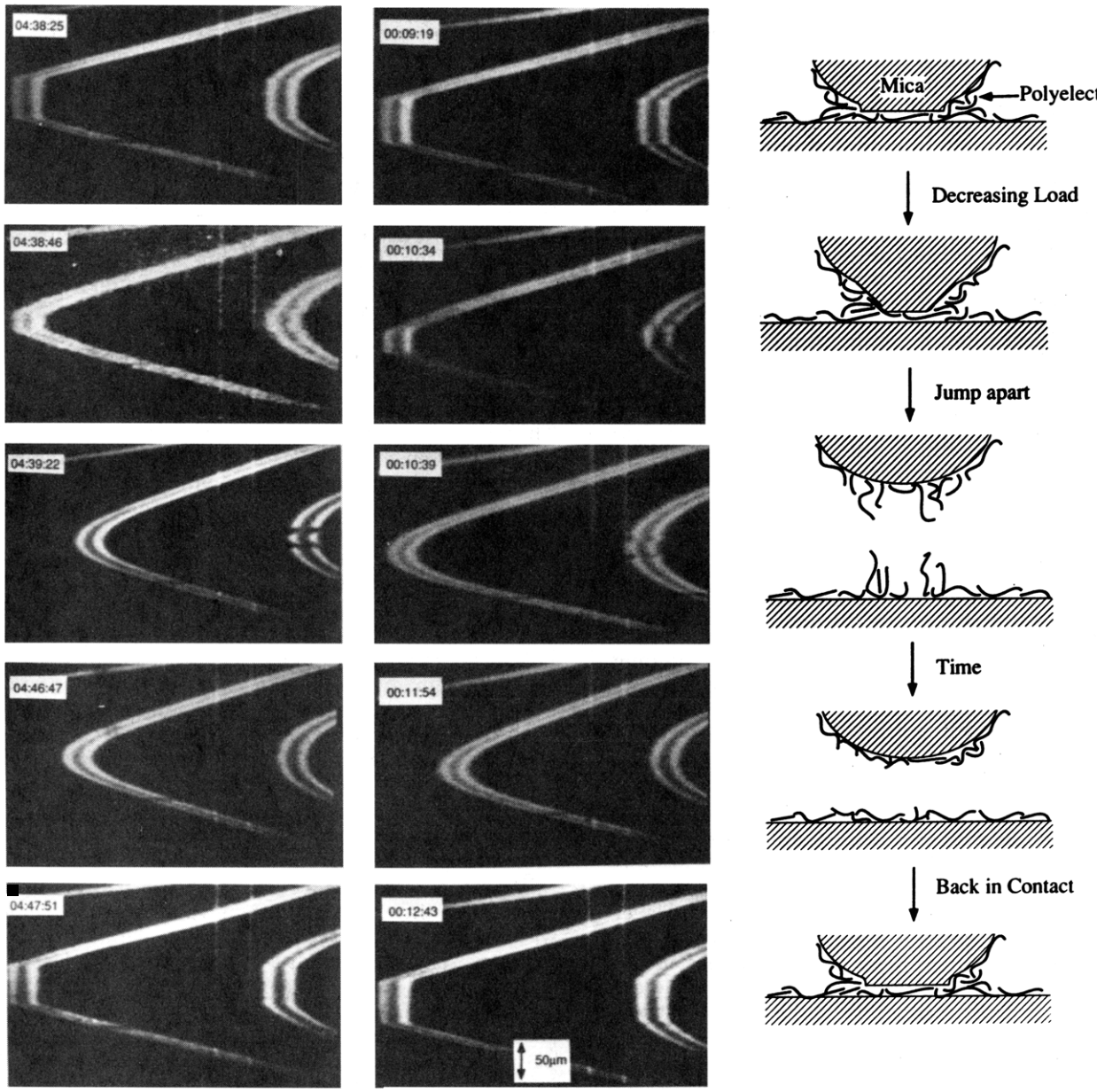

Figure 3. Spectrograms showing the FECO pattern obtained if two mica surfaces covered with polyelectrolyte monolayer are brought into contact and separated at rh ≈ 0% (left column) and rh ≈ 80% (center column) as well as schematics. An odd fringe is shown at the left, an even fringe at the right. Also, two lines of a calibration mercury pen-ray lamp can be seen. Top: Surfaces in contact; the even fringe appears to be broken due to the polymer annulus surrounding the contact area. Second row: This picture was taken just before the surfaces jumped apart. The contact area has almost reached its minimum value. Third row: The surfaces are separated in such a way as shown schematically in Figure 2. The wavelengths of the fringes coincide almost with contact wavelengths. The fringe with the wavelength of an even contact fringe has black holes at the position of the former meniscus. The odd fringe is homogeneous. This can be understood as a polyelectrolyte ring sitting on the surface. Fourth row: The polymers form again homogeneous monolayers covering the two mica surfaces; both fringes appear continuous. This process took 6–7 min at 0% rh and about 1 min at 80% rh. Bottom row: The surface are brought back into contact and the polyelectrolyte meniscus forms again.

niscus is there again. We have the impression that the meniscus grows during the first minutes, but our resolution is not good enough to quantify this observation (cf. Figure 3, bottom).

To estimate how many molecules are squeezed out of the contact area to form a polyelectrolyte meniscus, we determined the thickness of the polyelectrolyte layer left in the contact area with UV desorption according to ref 14. With the new batch of PAH, we found a thickness of ≈6 Å, which is clearly below the thickness of two monolayers and strongly supports our view that the polymers leave the contact area to form the meniscus.

Effect of Relative Humidity. The experiments shown in Figure 3 were performed at rh ≈ 0% (left column) and rh ≈ 80% (center column), respectively. For rh ≤ 80%, the effects are very similar: as soon as the surfaces contact, a polyelectrolyte meniscus forms. At rh ≈ 80%, the meniscus appears to be somewhat higher than at a lower rleative humidity, ≈8 nm.

However, the annealing time depends on the relative humidity. While at low relative humidities of ≈0% and ≈30% the annealing process took 6–7 min; at ≈80% the fringes appeared perfectly homogeneous after 1 min. This indicates an increased mobility of the polymer segments at high humidity, presumably due to water uptake.

Experiments performed at rh ≈ 100% are shown in Figure 5. The behavior of the polyelectrolyte monolay-

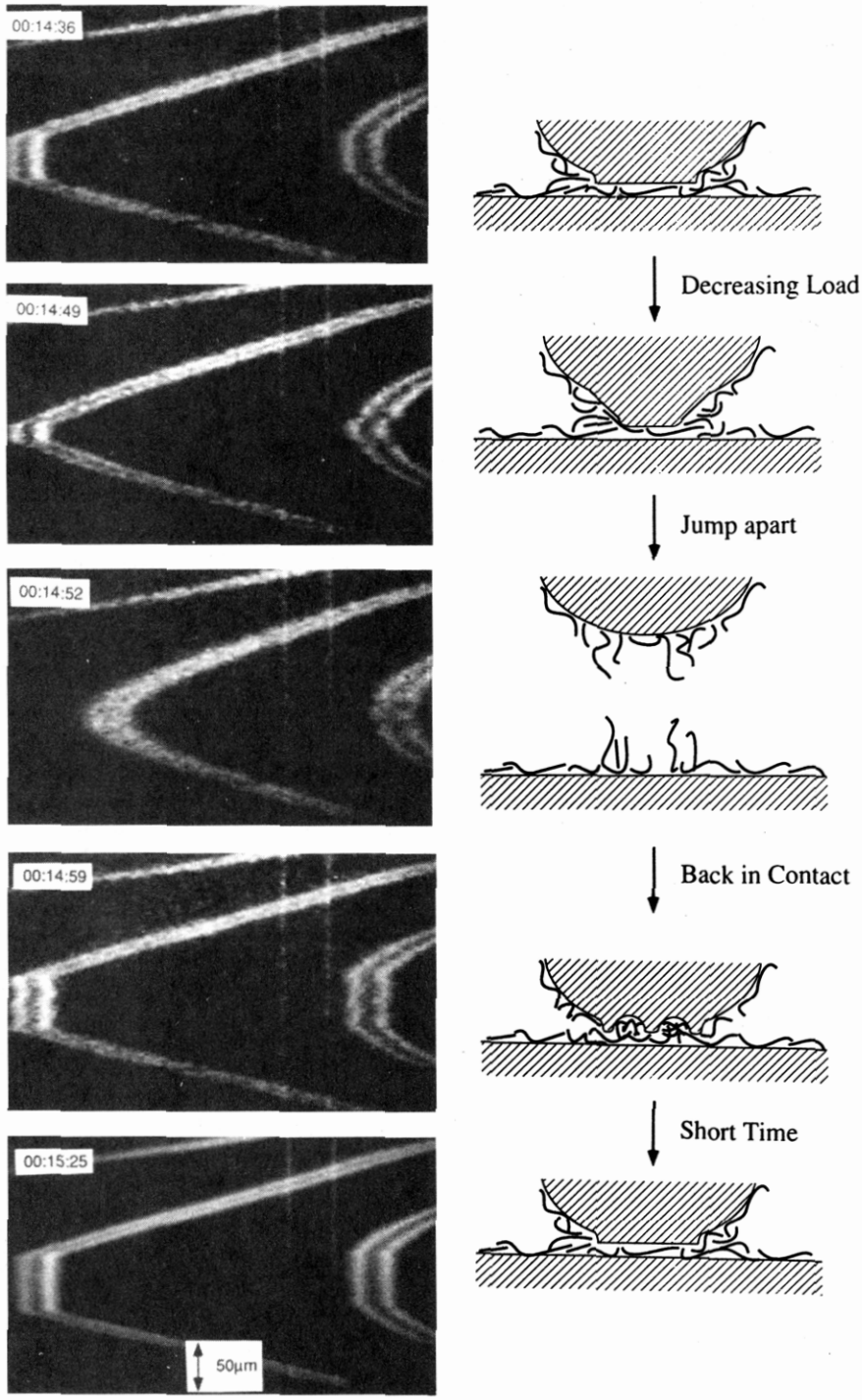

Figure 4. Spectrograms showing the FECO pattern produced by the formation of a polyelectrolyte meniscus from deformed monolayers (rh ≈ 80%) together with Schematics. Top: The surface in contact. Second row: The surfaces just before pull-off. Third row: The black holes in the right fringe indicate a polyelectrolyte annulus. Fourth row: The surfaces were immediately brought in contact. Both the left and the right fringes appear to bulge and wiggle. The movement takes at most 40 ms. Bottom row: The fringes are straight again.

ers changes drastically. If the surfaces contact, a polyelectrolyte annulus no longer grows around the contact area; instead a water meniscus is observed. A water annulus has distinctly different properties than a polyelectrolyte annulus: it grows with time, and after separation, all fringes appear homogeneous at all distances. The surfaces separate as soon as a sufficiently large tensile force is applied. After the rupture of a water meniscus, the remaining droplet spreads immediately and evaporates simultaneously; therefore no water ring exists. This is exactly the behavior we observe; we do not find any evidence for a movement of the polyelectrolyte monolayer.

These optical observations agree well with the forces necessary to separate the surfaces, which are given in Table 1. As long as our optical measurements indicate the formation of a polyelectrolyte annulus, the separation force is around 310 mN/m; when we observe a water meniscus, the separation force increases by a factor of 2.

If there is no adhesion between the surfaces in water, as in our case,[19] the force necessary to separate surfaces connected by a water meniscus is mainly determined by the Laplace pressure, $F_s = 4\pi R\gamma_L \cos\theta_r$. Here, γ_L is

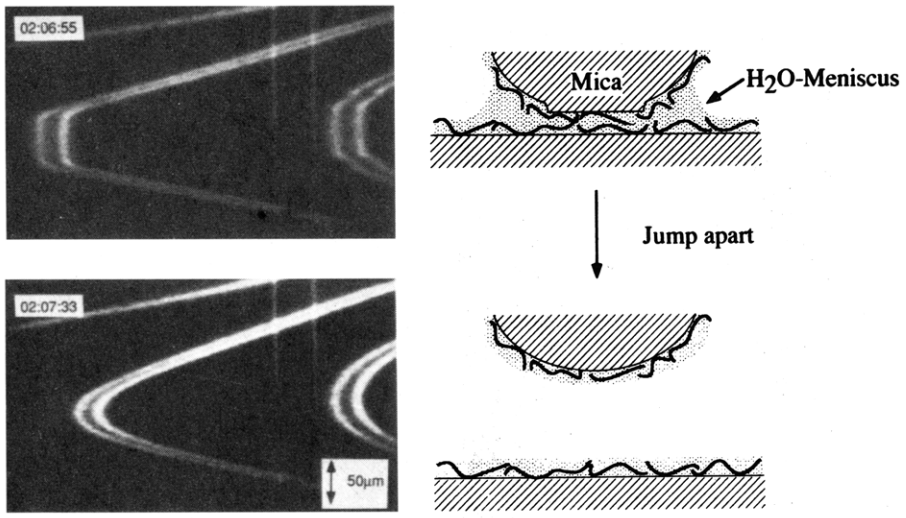

Figure 5. Spectrograms showing the FECO pattern obtained from the same surfaces as depicted in Figures 3 and 4 at rh ≈ 100% as well as schematics. Top: The surfaces are in contact and due to capillary condensation a water meniscus grows with time. Bottom row: On separation, the fringes are homogeneous indicating that the surfaces are uniformly covered with a presumably hydrated polyelectrolyte monolayer.

Table 1. Force (±10%) Necessary To Separate the Surfaces as a Function of the Relative Humidity (rh) for the Surfaces Whose Spectrograms Are Shown in Figures 3–5 and Results Deduced from the Growth and Annealing Properties

rh (%)	F_s/R [mN/m] (±10%)	nature of meniscus
0	302	polyelectrolyte
30–35	300	polyelectrolyte
81	330	polyelectrolyte
100	603	water

the surface tension of the liquid, and θ_r is the receding contact angle between the surface and the liquid; we have $\cos \theta_r = 1$. Considering the measured separation force given in Table 1 together with the contact angle measurements described below, we obtain a surface tension of water $\gamma_L \approx 50$ mN/m, which is obviously too low. As in our previous work on capillary condensation of surfactant-covered mica surfaces,[11] we find that $F_s = 3\pi R\gamma_L$ leading to $\gamma_L \approx 67$ mN/m, describes our experimental data rather well; however, we have no strong theoretical arguments for this equation. To our knowledge, only Fogden and White[18] have derived a separation force $F_s = 3\pi R\gamma_L$ rather than $F_s = 4\pi R\gamma_L$ for a capillary condensed meniscus. They base their equations on a strong solid–solid adhesion and a very small radius of the water meniscus. Obviously, both assumptions do not apply for our experiments. Therefore, we have to conclude that the adsorbed monolayer yields to the strong tensile stresses. This leads to a small additional deformation of the adsorbed monolayers at the three-phase line and presumably reduces the force necessary to separate the surfaces.

First Movement of the Monolayer. If the surfaces are brought into contact for the first time, we do not always observe the polymer meniscus (and the black holes) immediately. With a few experiments, it is necessary to bring the surfaces three or four times in contact or let them sit there for 10 min. However, once the polymer annulus forms (and the black holes appeared, which turned out to be an even better indication of polyelectrolyte movement), the experiments could be repeated several times.

Also, we would like to mention that the polymer meniscus could be observed best if the radius of the sphere was $R = 1.5–2$ cm. For smaller radii, the only remarkable feature was the edge shape of both the odd and even fringes. The formation of the polyelectrolyte meniscus was deduced from the appearance of the black holes after separation. The formation of the polymer meniscus is due to polyelectrolyte transport from the center of the contact area toward the edges, and it is intuitive that for larger contact areas (resulting from larger sphere radii) the meniscus is more pronounced.

Photobleaching on an Isolated Monolayer. To determine if the monolayer movement is caused by lateral diffusion or by convective flux (driven by the gradient in surface energy), bleaching experiments on isolated FITC-labeled PAH monolayers were performed. These were executed as follows: A thin sheet of mica is glued on a microscope slide, the polyelectrolyte monolayer is prepared as described before, and the slide is mounted in the microscope. Then the iris diaphragm between the light source and the sample is closed as much as possible, illuminating a circle with diameter of about 120 μm. If this circle is exposed to the intense light of the excitation lamp for about 5–10 min, the dye is chemically destroyed (bleached) and no longer emits fluorescence radiation. If the iris diaphragm is opened again, in the fluorescence configuration the bleached spot appears to be dark, as shown in Figure 6. Its boundary follows the detailed shape of the iris diaphragm. The shape is unchanged after 30 min; no fluorescence recovery occurs. Obviously, the polyelectrolytes within the monolayer are immobilized; the diffusion coefficient is almost zero. Increasing the relative humidity had no effect on the lateral diffusion coefficient.

We performed the same experiment with a PAH monolayer on a glass slide; there, too, no measurable diffusion occurs. As may be expected, no diffusion is found if a PSS layer is sitting on a PAH layer.

Wetting Experiments. To find out if the high surface energy plays such an important role on the spreading properties of the polyelectrolyte as our SFA experiments suggest, we performed some wetting experiments. To reduce contamination of the mica surface, the wetting experiments were performed in a clean bench. The thin mica sheet (glued onto a microscope slide) was half immersed into a solution of the FITC-labeled polyelectrolyte. It stayed there for 5 h. Then the mica sheet was removed from the solution, dried,

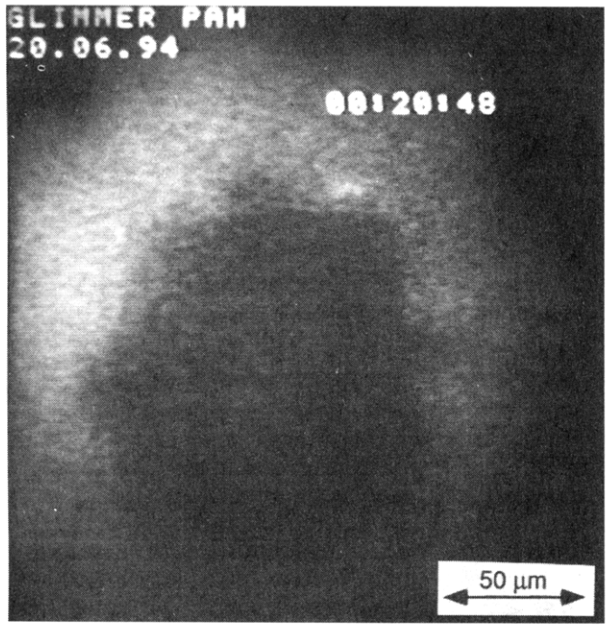

Figure 6. A bleached spot on a FITC-labeled PAH monolayer adsorbed onto mica as observed with a microscope in the flourescence configuration. To bleach the monolayer locally, the iris diaphragm was closed as much as possible and the remaining spot was illuminated from 5–10 min. The fact that photobleaching is feasible and the stability of the bleaching spot over 30 min indicate that the diffusion coefficient within the PAH monolayer is almost zero.

and inspected with the microscope. A monolayer covering the complete mica surface was found; the piece of mica which was not immersed into the solution was about 3 cm long. Obviously, the polyelectrolyte adsorbed at the mica/water interface and then migrated along the mica/air interface. We found no difference in the contact angle with water or in the fluorescence intensity for the two differently prepared sections of the monolayer.

These experiments suggest that the diffusive transport is almost zero. However, there is flow; the polymers slip along the surface driven by the gradient in surface energy. Apparently, the movement within the flat polymer coils is much less than the movement of the whole coils relative to the surface.

In the SFA, the formation of a polyelectrolyte depleted the monolayer in the contact area. After separation of the surfaces, part of the mica surface is exposed to the nitrogen atmosphere, leading to an increase of the surface energy. This change in surface energy is the driving force of the mechanically disturbed monolayer to anneal.

Influence of the Polyelectrolyte Batch. With a new batch of PAH, the mobility described above could only be observed if the pH of the polyelectrolyte solution was reduced to ≈2.5 with HCl. The attractive force between the polyelectrolyte segments and the mica depends on the charge of the polyelectrolyte monomers as well as the adsorbed counterions, parameters which are apparently not well controlled during the synthesis. Yet, we observe again the black holes; however, their width is reduced (≈1 μm). Quantitatively, the results are different: the force necessary to separate the surfaces connected by a polyelectrolyte meniscus is much larger than the one given in Table 1 and decreases by a factor of 2 when a water meniscus is observed. Qualitatively, the results are the same: when surfaces connected by a polyelectrolyte meniscus are separated, their movement is rather sluggish and after application of a sufficient tensile force one has to wait about 1 s until the surfaces eventually jump. The nature of the meniscus determines the force necessary to separate the surfaces; the influence of the relative humidity is negligible. Again, the black holes anneal within minutes.

A Polyelectrolyte Bilayer. In order to gain insight into the effects of chain entanglement, we prepared a polymer bilayer, the first layer being PAH (as before), and the second PSS. The thickness was determined as before: a PSS solution was placed in the SFA between the PAH-covered mica surfaces, and we waited 0.5 h until the adsorption was completed. Then the surfaces were pressed together until the flattening was comparable to the one observed in air. Thus, we determined that each bilayer was 1.4–1.6 nm thick. These numbers are in good agreement with the X-ray experiments on polyelectrolyte multilayers.[5]

The results obtained with bilayers in air are shown in Figure 7. In general, surfaces covered with polymer bilayers lead to more fuzzy fringes, indicating an increased surface roughness. Here, thinner mica is used than in the experiments shown before; therefore only the even fringe can be seen. On separation, we observe again the familiar black holes. However, they no longer disappear and are unchanged after 48 h of waiting, almost independent of humidity.

The third picture in the row was taken after the surfaces were brought in and out of contact several times quite quickly. Such a mistreatment favors the buildup of plastic deformation of the polyelectrolyte bilayer. Note in the third picture in this series a little bright spot indicating the height of the polyelectrolyte ring (or part of the ring) sitting on the surfaces. To show both the bright spot and the tip of the fringe in our field of view, we had to change the distance from the position of maximum field enhancement at the mica surface. Then one no longer sees two black holes but one big hole. We do not understand the reasons for this effect; presumably it is related to light scattering and surface roughness.

Even this severe deformation did not anneal anymore. Yet, when we brought the surfaces back in contact, the surfaces wiggled a bit, and then the contact line appeared to be perfectly smooth, as before. Apparently, the polyelectrolyte bilayer no longer anneals; however, it undergoes very easily plastic deformations.

The thickness of the remains of the two polyelectrolyte bilayers trapped between the surfaces while the contact area was surrounded by a polyelectrolyte meniscus was again determined by UV desorption according to ref 14. We found an overall thickness of 2.2 ± 0.6 nm. Therefore, the polyelectrolyte bilayer can be deformed and partly depleted without any exposure of the mica surface to the nitrogen atmosphere. Therefore, no gradient in the surface energy occurs, and the surfaces do not anneal.

Conclusions and Implications

If capillary growth between modified surfaces of a solid is to be investigated, one has to consider rearrangements of any molecules physisorbed onto the surfaces. If the surfaces contact, the movement of those molecules is determined both by the surface energy and by mechanical stresses. Polyelectrolyte monolayers are quite convenient for such studies since their rearrangement can be observed easily. We always observe a meniscus surrounding the contact area. However, at

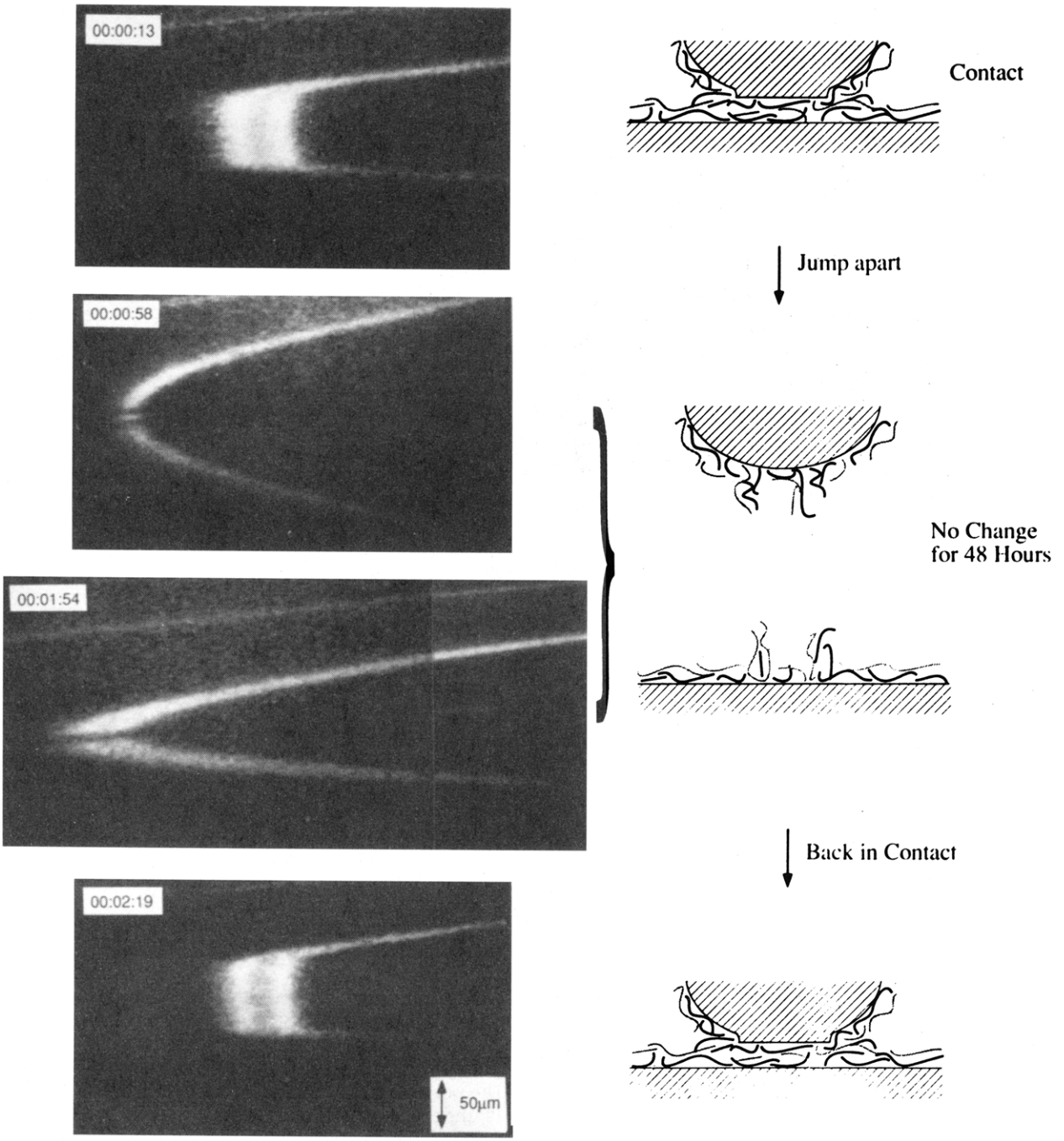

Figure 7. Spectrograms showing a FECO produced by a deformed polyelectrolyte bilayer at ambient conditions together with schematics. Top: An even contact fringe is shown. Second row: After separation the black holes are observed. Third row: Moving the fringes a bit toward the left, away from the contact wavelength of the even fringe, one can no longer observe the two black holes, but rather one hole. Yet, the tip of the polymer ring can be seen (the little white spot at the center). Such a severe deformation as shown in this picture was only seen after several contacts and separations. It did not anneal within 48 h. Bottom row: If the surfaces are brought into contact again, the fringes appear homogeneous.

low relative humidities, it consists mainly of polyelectrolyte; at rh $\approx$ 100% it consists of water. The polyelectrolyte and the water meniscus can be distinguished by their growth and annealing properties. The nature of the meniscus correlates extremely well with the force necessary to separate the surfaces. After separation, the mechanically induced deformations of the polyelectrolyte monolayers anneal. Obviously, the gradient of the surface energy leads to a force strong enough to move a monolayer, since a sheet of mica half immersed into polyelectrolyte solution is found to be completely covered with a monolayer (after an appropriate amount of time). Photobleaching experiments indicate that the diffusion coefficient of chains within a monolayer is extremely low. Therefore we conclude that the chains move in the direction of the flux without much movement of the chain segments relative to each other.

Acknowledgment. First of all, we would like to thank Johannes Schmitt; his explanations on the entangled subject of polyelectrolytes were a great help to the project. We had various discussions with Prof. Helmuth Möhwald and thank him for his support. In connection with the SFB 262, we enjoyed a rather enlightening talk with Dr. Thomas Vilgis. Finally, discussions with Dr. Gero Decher had always their special charm ("I can't believe you measure that!"). We appreciate that Frank Essler dialyzed the PSS. C.A.H.

acknowledges financial support of the Deutsche Forschungsgemeinschaft (He 1616/4-1) as well as the BMFT (F + E-Vorhaben 13N6284) for the camera. K.L. is indebted to the project He 1616/5-1 of the Deutsche Forschungsgemeinschaft.

Appendix

If two flat homogeneous surfaces in air contact, spontaneous flattening occurs due to adhesion. The FECO fringes are no longer rounded, but their center is a straight line, whose length corresponds to the diameter of the contact area. At the boundary of the contact area, the distances between the surfaces are still small, and eqs 2 and 3 together with $n_{Gl} = 1.58$ and $n = 1$ (for air) apply. The shift of the odd fringes is proportional to $n_{G1} = 1.58$, whereas the shift of the even fringes is proportional to $n^2/n_{G1} = 0.63$. Therefore, above and below the straight line, the odd fringes appear to have sharp edges, while the even fringes seem to be more rounded. For instances, in Figure 3 the fringe at the left is an odd fringe, and the one at the right an even one.

Israelachvili[13] gives the general equation for constructive interference for a symmetrical five-layer interferometer:

$$\begin{aligned}\tan(knD) = (1 - r_1^2)\{&\sin(2k(n_F D_F + n_{Gl} D_{Gl})) - \\ &2r_2 \sin(2kn_F D_F) + r_2^2 \sin(2k(n_F D_F - n_{Gl} D_{Gl}))\} \times \\ &[2r_1\{1 - 2r_2 \cos(2kn_{Gl} D_{Gl}) + r_2^2\} - \\ &(1 + r_1^2)\{\cos(2k(n_F D_F + n_{Gl} D_{Gl})) - \\ &2r_2 \cos(2kn_F D_F) + r_2^2 \cos(2k(n_F D_F - n_{G1} D_{G1}))\}]^{-1}\end{aligned} \quad \text{(A1)}$$

For our experiments, D_{G1} and n_{G1} are the thickness and refractive index of the mica, D_F and n_F are the respective values of the polyelectrolyte monolayer, and D and n describe the air gap. Also, the following abbreviations are used:

$$r_1 = \frac{n_F - n}{n_F + n} \quad \text{and} \quad r_2 = \frac{n_{Gl} - n_F}{n_{Gl} + n_F} \quad \text{(A2)}$$

For a given distance D, eq A1 is satisfied by those values $k = 2\pi/\lambda$ that appear as bright fringes. Then, Israelachvili[13] proceeds to describe the case when both D_F and D are very thin. In this case, the resonance wavelength $\lambda_m = \lambda^0{}_m + \Delta\lambda$ is shifted only slightly compared to $\lambda^0{}_m$, the resonance wavelength of a one-layer interferometer consisting of contacting mica sheets and defined according to eq 1. With the assumptions that D_F, D, and $\Delta\lambda$ are all very small, together with some trigonometric relationships ($\cos(\pi + \alpha) = -\cos(\alpha)$, $\sin(\pi + \alpha) = -\sin(\alpha)$) and eq 1, one obtains

$$D = m\frac{\Delta\lambda}{2n_{Gl}} - 2D_F, \quad \text{for } m \text{ odd} \quad \text{(A3)}$$

and

$$Dn^2 + m\frac{\Delta\lambda n_{Gl}}{2} - 2D_F n_F^2, \quad \text{for } m \text{ even} \quad \text{(A4)}$$

Again, as for the three-layer interferometer, we find for the odd fringes no influence of the refractive index of the media between the mica sheets, whereas for the even fringes this influence is pronounced. This is due to the fact that at the center of the cavity the light field is either zero or at maximum (cf. Figure 2).

Now let us consider an interferometer where the surfaces are separated so far that a resonance fringe λ_M almost coincides with a contact fringe $\lambda^0{}_m$; i.e.

$$\lambda_M = \lambda^0{}_m + \partial\lambda \quad \text{with } M > m \text{ and } \partial\lambda \to 0 \quad \text{(A5)}$$

Note that $M > m$, $\lambda^0{}_M$, and $\lambda^0{}_m$ may differ considerably; i.e., the air gap D may be quite large.

If we insert λ_M into the right side of eq A1, we obtain the same power series as before when we derived eqs A3 and A4. $\lambda^0{}_M$ and the order of the fringe M have no impact in this approximation. Yet, the distance between the mica sheets is increased. The left side of eq A1 is an equation of the type $\tan(x) = a$. In principle, it has an infinite number of solutions for x differing by multiples of π. Let us call D_0 that solution to eq A1 whose absolute value is smallest. Then all other solutions for D differ by multiples of $\lambda/(2n)$.

Experimentally it is obvious that the air gap between the surfaces increases continuously. Therefore we obtain for $\lambda_M = \lambda^0{}_m + \partial\lambda$ at distances $D = (\lambda_M/2n)(M - m) + D_0$ the following approximations:

$$D_0 = m\frac{\partial\lambda}{2n_{Gl}} - 2D_F, \quad \text{for } m \text{ odd} \quad \text{(A6)}$$

$$D_0 n^2 = m\frac{\partial\lambda n_{Gl}}{2} - 2D_F n_F^2, \quad \text{for } m \text{ even} \quad \text{(A7)}$$

Note that the refractive index of the thin film does not influence the wavelength shift for wavelengths which almost coincide with odd contact fringes. In contrast, a quadratic relationship is found for those wavelengths which almost equal even contact fringes. This approximation works best if (i) the refractive indices of the three layers between the mica sheets resemble the refractive index of mica, (ii) $M - m = 1$ or $M - m = 2$, and (iii) m is rather small.

References and Notes

(1) Daillant, J.; Benattar, J. J.; Leger, L. *Phys. Rev. A* **1990**, *41*, 1963.
(2) de Gennes, P.-G. *Rev. Mod. Phys.* **1985**, *57*, 827.
(3) Migler, K. B.; Hervet, H.; Leger, L. *Phys. Rev. Lett.* **1993**, *70*, 287.
(4) Carmesin, I.; Kremer, K. *J. Phys. Fr.* **1990**, *51*, 915.
(5) Decher, G.; Schmitt, J. *Prog. Colloid Polym. Sci.* **1992**, *89*, 160.
(6) Chen, Y. L.; Gee, M. L.; Helm, C. A.; Israelachvili, J. N.; McGuiggan, P. M. *J. Phys. Chem.* **1989**, *89*, 7057.
(7) Israelachvili, J. N. *Intermolecular and Surface Forces*; Academic Press: London, 1991.
(8) Christenson, H. K.; Yaminski, V. V. *Langmuir* **1993**, *9*, 2448.
(9) Horn, R. G.; Israelachvili, J. N.; Pribac, F. *J. Colloid Interface Sci.* **1987**, *115*, 480.
(10) Johnson, K. L.; Kendall, K.; Roberts, A. D. *Proc. R. Soc. London, Ser. A.* **1971**, *324*, 301.
(11) Chen, Y. L.; Helm, C. A.; Israelachvili, J. N. *J. Phys. Chem.* **1991**, *95*, 10736.
(12) Nargessi, R. D.; Smith, D. S. *Methods Enzymol.* **1986**, *122*, 67.
(13) Israelachvili, J. N. *J. Chem. Soc., Faraday Trans. 2* **1973**, *69*, 1729.
(14) Chen, Y. L.; Helm, C. A.; Israelachvili, J. N. *Langmuir* **1991**, *11*, 2694.
(15) Fisher, L. R.; Israelachvili, J. N. *Colloids Surf.* **1981**, *3*, 303.
(16) Mächtle, P.; Müller, C.; Helm, C. A. *J. Phys. II Fr.* **1994**, *4*, 481.
(17) Ramsden, J. J.; Lvov, Y.; Decher, G. *Thin Solid Films* **1995**, *254*, 246.
(18) Fogden, A.; White, L. R. *J. Colloid Interface Sci.* **1990**, *138*, 414.
(19) Lowack, K.; Helm, C. A., to be published.

MA946007G